encit 2020

ABCM Associação Brasileira de Engenharia e Ciências Mecânicas

18th Brazilian Congress of Thermal Sciences and Engineering
November 16-20, 2020 (Online)

ENC-2020-0443
NUMERICAL SIMULATION OF FLOW ON SYMMETRICAL AIRFOIL USING AN IMERSPEC METHODOLOGY

Lucas Gabriel Pereira Silva
Mariana Fernandes dos Santos Villela
Universidade Federal de Pernambuco – Campus Acadêmico do Agreste, Caruaru-PE
lucas.gabrielpereira@ufpe.br, mariana.villela@ufpe.br

Felipe Pamplona Mariano
Universidade Federal de Goiás, Escola de Engenharia Elétrica, Mecânica e de Computação, Laboratório de Engenharia Térmica e de Fluidos – LATEF, Goiânia-GO
fpmariano@ufg.br

Abstract. *The IMERSPEC methodology results from the fusion of two methodologies for solution of Computational Fluid Dynamics problems (CFD): the Fourier pseudospectral method (FPS) and the immersed boundary method (IB). The first one stands out due to the high order of convergence (spectral), its high accuracy (machine error) and its high computational efficiency (absence of linear systems to be solved). However, the FPS has limited application to periodic problems. The IB method is characterized by the ability to model and solve problems of any complexity, mobility and geometric deformability, using cartesian meshes. The fusion of these methods allows to eliminate the FPS periodicity restriction and the partial maintenance of its order of convergence and its precision. The purpose of this research is the application of the IMERSPEC methodology for the solution of differential models applied to the fluid-structure interaction, focusing on mathematical modeling and numerical investigation of the flow over a symmetrical airfoil (NACA0012). The analysis of the flow was made for low Reynolds number (Re = 1000) for different angles of attack. As the angle of attack increases, the instability of the flow and the presence of vortices in the streamlines are noted, due to the separation of the boundary layer on the upper surface of the airfoil. The variation of the aerodynamic coefficients in relation to the angle of attack can also be seen, the lift coefficient, which has a maximum value at a certain angle, known as the stall angle, and the drag coefficient increases as the angle of attack increases.*

Keywords: *IMERSPEC, flow over airfoil, computational fluid dynamics.*

1. INTRODUCTION

Airfoils have different applications, *e.g.*, high-lift airfoils are intended for applications that require large lift forces and low Reynolds number. They are used in competition aircraft, cargo aircraft and some types of gliders. The focus of the present work is NACA series airfoils in laminar flow. They have geometric characteristics that favor the permanence of the boundary layer along the airfoil, indicated for low Reynolds numbers. They are used as turbocharged blades and some types of gliders. Supercritical airfoils are normally used in Unmanned Aerial Vehicle, also known as UAVs, and in wind turbines with reasonable lift and low drag in order to increase the efficiency of wind power generation.

The choice of the ideal airfoil shape for each application can be very complex, so it's not always possible to solve problems analytically. Therefore, over the years, numerous studies on numerical simulations in airfoil have emerged. In Giannakoglou's work (2002) stochastic optimization methods (randomly determined process) were used to find optimum aerodynamic shapes. Shahrokhi and Jahangirian (2007) studied the effect of airfoil shape parameterization on optimum design for high Reynolds numbers. McNaughton *et al.* (2014) propose a two-dimensional numerical investigation of a vertical axis wind turbine, analyzing two different turbulence models.

Therefore, the purpose of the present research is the application of the IMERSPEC methodology (Mariano, 2011) for the solution of differential models applied to the fluid-structure interaction, focusing on mathematical modeling and numerical investigation of the flow over an NACA series airfoil.

The IMERSPEC methodology results from the fusion of two other methodologies for solving Fluid Dynamics problems: the Fourier pseudospectral method (FPS) (Canuto *et al.*, 2006), (Canuto *et al.*, 2007) and the immersed boundary (IB) method (Peskin, 1972). The first one stands out due to the extremely high order of convergence (spectral), its accuracy (machine error) and its high computational efficiency (absence of linear systems to be solved). The IB method is characterized by the ability to model and solve problems of any complexity, mobility and geometric deformability

using cartesian meshes. The fusion of these methods allows to eliminate the FPS periodicity restriction, partially maintaining its order of convergence and accuracy in addition to being applicable to any type of geometry.

2. METHODOLOGY

This section presents the synthesis of the methodology used in Monteiro *et al*. (2019) and Mariano (2011). Specifically describes the Navier-Stokes equations, that models fluid flow, and the mathematical formulation for immersed boundary method to impose the boundary conditions in physical space. After that, it presents the transformed from physical model to Fourier spectral space.

2.1 Mathematic model for the fluid

To analyze the flow over symmetrical airfoils, the Navier-Stokes equations are used, which is a set of equations that models the movement of fluids to Newtonian and incompressible fluids flow in two-dimensional domain. The Navier-Stokes equations (Eq. (1)) and the continuity equation (Eq. (2)) are presented in theirs tensorial form:

$$\frac{\partial u_l}{\partial t} + \frac{\partial (u_l u_j)}{\partial x_j} = -\frac{\partial p}{\partial x_l} + \nu \frac{\partial^2 u_l}{\partial x_j \partial x_j} + f_l, \tag{1}$$

$$\frac{\partial u_j}{\partial x_j} = 0, \tag{2}$$

where $\mathrm{p} = p^*/\rho + \mathrm{gz}$; p^* is the static pressure in [N/m^2]; z is the vertical dimension aligned with the gravity vector $\vec{g}$; $u_l[m/s]$ are the velocity components, the index l represents direction and $l = 1,2$ for two-dimensional problems; $f_l = f_l^*/\rho$; f_l^* is the source term of force in [N/m^3]; ρ is the density in [kg/m^3]; ν is the kinematic viscosity in [m^2/s].

The source term, f_l, enables that the Eulerian field perceives the presence of solid interface (Enriquez-Remigio and Silveira Neto, 2007) and it is given by Eq. (3).

$$f_l(\vec{x},t) = \begin{cases} F_l(\vec{x}_k,t) & if \quad \vec{x} = \vec{x}_k \\ 0 & if \quad \vec{x} \neq \vec{x}_k \end{cases}, \tag{3}$$

where $\vec{x}$ is the position of the particle in the fluid and $\vec{x}_k$ is the position of a point in solid interface (Fig. 1).

The boundary conditions are periodic in all directions in Eulerian domain, Ω_B, as showed in Fig. 1, due to imposition given by Fourier pseudospectral method properties. The boundary condition is imposed by direct forcing method in Γ_{BC}, and the boundary conditions of bodies immersed in flow, represented by Γ_i in Fig. 1 (Mariano, 2011).

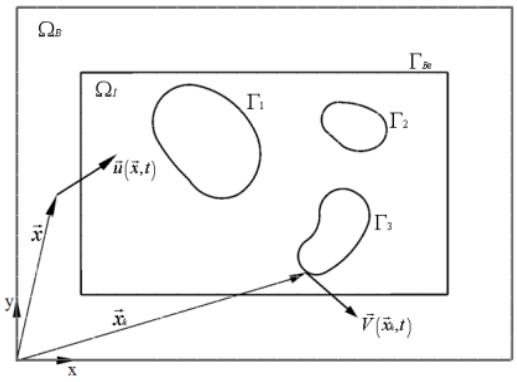

Figure 1. Schematic representation of eulerian and lagrangian domain (Mariano, 2011).

By Equation. (3) can be concluded that the field $f_l(\vec{x},t)$ is discontinuous, which can be numerically solved only when there is coincidence point in the interface domain with the points of the fluid domain. In the cases there is no coincidence, very frequently in the complex geometries, it is necessary to distribute the function $f_l(\vec{x},t)$over its neighborhoods. For this, lagrangian force field $F_l(\vec{x}_k,t)$ is calculated and after that distributed and, then, the information is transmitted for Eulerian domain,and this way the fluid perceives the presence of the geometry. These functions can be found in Griffith and Peskin, (2005).

2.2. Mathematic model for the immersed interface

In the mathematical modeling by the immersed boundary method, there are particular characteristics that must be defined, which are done in three stages: treatment of the eulerian and lagrangian domains, the transfer of information between these domains and, finally, the calculation of lagrangian force.

The calculation domains mentioned are worked simultaneously in the IB method, the eulerian domain (Ω), cartesian and fixed, where the equations for the fluid are solved, Eq. (1) and Eq. (2), and the lagrangian domain (Γ) (Fig. 2), which represents the interface immersed in the flow. It should be mentioned that the equations for the fluid are solved for the entire eulerian domain, even in the region inside the lagrangian domain.

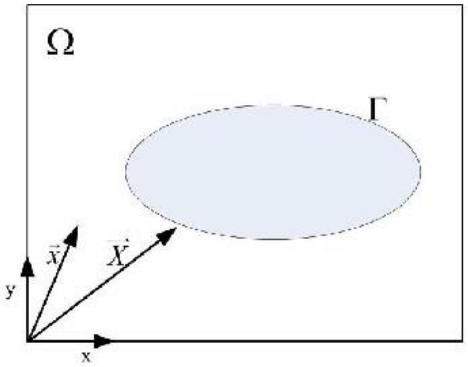

Figure 2: Eulerian domain (Ω) and lagrangian domain (Γ).

Since the lagrangian domain is independent from the eulerian, it is possible to simulate flows over complex geometries even using a cartesian domain.

The next step is to establish communication between the domains. The immersed boundary method consists of adding the source term (f_i), which the boundary conditions are indirectly modeled according to Eq. (1) and Eq. (2). The Lagrangian force field is calculated by direct forcing method was proposed by Uhlmann (2005). This method does not need to use *ad-hoc* constants and allows to model non-slip condition on immersed interface (Monteiro et al., 2019). The Lagrangian force $F_l(\vec{x}_k,t)$ is obtained through momentum conservation equation (Eq. (1)) given by Eq. (4):

$$F_l(\vec{x}_k,t)=\frac{\partial u_l}{\partial t}(\vec{x}_k,t)+\frac{\partial}{\partial x_j}(u_l u_j)(\vec{x}_k,t)+\frac{\partial p}{\partial x_l}(\vec{x}_k,t)-\nu\frac{\partial^2 u_l}{\partial x_j \partial x_j}(\vec{x}_k,t). \tag{4}$$

The $u_l(\vec{x}_k,t)$ and $p(\vec{x}_k,t)$ are obtained by interpolation of Eulerian points near the immersed interface of velocities and pressure, respectively. Then, for Lagrangian points, x_k, at the immersed boundary:

$$F_l(\vec{X}_k,t)=\frac{u_l(\vec{x}_k,t+\Delta t)-u_l^*(\vec{x}_k,t)+u_l^*(\vec{x}_k,t)-u_l(\vec{x}_k,t)}{\Delta t}+RHS_l(\vec{x}_k,t), \tag{5}$$

where u^* is a temporary parameter (Wang, *et al.* 2008), Δt is the time step and $RHS_l(\vec{x}_k,t)=\frac{\partial}{\partial x_j}(u_l u_j)(\vec{x}_k,t)+\frac{\partial p}{\partial x_l}(\vec{x}_k,t)-\nu\frac{\partial^2 u_l}{\partial x_j \partial x_j}(\vec{x}_k,t)$.

The Eq. (5) is solved by Eqs. (6) and (7) at same time step:

$$\frac{u_l^*(\vec{x}_k,t)-u_l(\vec{x}_k,t)}{\Delta t}+RHS_l(\vec{x}_k,t)=0, \tag{6}$$

$$F_l(\vec{x}_k,t)=\frac{u(\vec{x}_k,t+\Delta t)-u_l^*(\vec{x}_k,t)}{\Delta t}, \tag{7}$$

where $u(\vec{x}_k,t+\Delta t)=U_{Fl}$ is the velocity of immersed boundary.

The Equation (6) is solved in the Eulerian domain in the Fourier spectral space, *i.e*, the solution of Eq. (1) with $f_l=0$. After that, $u_l^*(\vec{x},t)$ is interpolated for Lagrangian domain and obtained $u_l^*(\vec{x}_k,t)$. Then it is calculated Eq. (7) and $F_l(\vec{x}_k,t)$ is distributed for Eulerian mesh. Finally, the velocity is update by Eq. (8):

$$u_l(\vec{x},t+\Delta t)=u_l^*(\vec{x},t)+\Delta t.f_l. \tag{8}$$

2.3. Fourier Pseudo-Spectral Method

Applying the Fourier transform (Villela, 2015) in Eq. (1) and Eq. (2), the set of equations below is obtained:

$$\frac{\widehat{\partial u_i}}{\partial t} + \frac{\widehat{\partial (u_i u_j)}}{\partial x_j} = -\frac{\widehat{\partial p}}{\partial x_i} + \nu \widehat{\frac{\partial^2 u_i}{\partial x_j \partial x_j}} + \hat{f}_i \tag{9}$$

$$\frac{\widehat{\partial u_j}}{\partial x_j} = 0 \tag{10}$$

From the properties of the Fourier transform (Villela, 2015), it is obtained from Eq. (11) that:

$$ik_i \widehat{u_i} = 0 \tag{11}$$

Based on linear algebra, it is known that the scalar product between two vectors is zero when they are orthogonal to each other, therefore, from Eq. (11), the transformed velocity vector $\hat{u}(\vec{k}, t)$ is orthogonal to the wavenumber vector $\vec{k}$. The π plane is defined, perpendicular to the vector, which contains the velocity vector transformed according to Fig. 3.

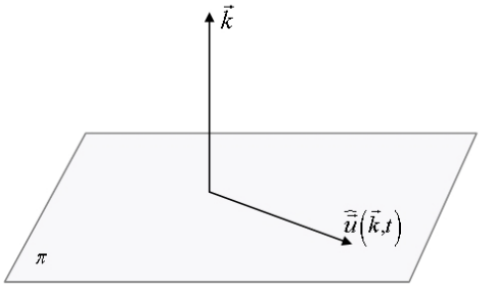

Figure 3: π plane. (Mariano, 2011)

Analyzing each term in Eq. (9) and applying the properties of the Fourier transform in relation to the π plane:

$$\frac{\partial \hat{u}_l^*}{\partial t} + ik_j \widehat{u_l^* u_j^*} = -ik_l \hat{p} - \nu k^2 \hat{u}_l^* + \hat{f}_l, \tag{12}$$

where k^2 is the square norm of wave number vector, *i.e.*, $k^2 = k_j k_j$. and $i = \sqrt{-1}$.

In agreement of the plane π definition, each one of the terms of Eq. (12) assumes a position related to it: the transient term and the viscous term belong to the plane π. The gradient pressure term is perpendicular to plane π and the non-linear and force terms, a priori, they are not known in which position it can be found in relation to plane π (Mariano, 2011 and Monteiro *et al.*, 2019). By joining the terms of Eq. (12) and observing the definition of plane π:

$$\underbrace{\left[\frac{\partial \hat{u}_l^*}{\partial t} + \nu k^2 \hat{u}_l^*\right]}_{\in \pi} + \underbrace{\left[ik_j \widehat{u_l^* u_j^*} + \hat{f}_l + ik_l \hat{p}\right]}_{\in \pi} = 0. \tag{13}$$

To solve Eq. (13) is needed that the non-linear and the force field terms are over plane π. For that, it is utilized projection tensor definition (Canuto *et al.*, 2007), which projects any vector over it. Therefore, applying this definition on the right-hand side of the sum done in Eq. (13):

$$\left[ik_j \widehat{u_j^* u_l^*} + ik_l \hat{p}\right] = \wp_{lm}\left[ik_j \widehat{u_m^* u_l^*} + \hat{f}_l\right]. \tag{14}$$

The term of the gradient pressure is orthogonal to plane π, then, it is zero after to be projected, uncoupling from calculates of Navier-Stokes equations in the spectral space. The pressure field can be recovered at the post-processing manipulating Eq. (14) (Canuto *et al.*, 2006).

Therefore, the momentum equation in the Fourier space, using the method of the projection, assumes the following form:

$$\frac{\partial \hat{u}_l^*(\vec{k},t)}{\partial t} + \nu k^2 \hat{u}_l^*(\vec{k},t) = -ik_j \wp_{lm}\left[\hat{f}_l + \int_{\vec{k}=\vec{r}+\vec{s}} \hat{u}_m^*(\vec{r},t)\hat{u}_l^*(\vec{k}-\vec{r},t)d\vec{r}\right]. \tag{15}$$

Non-linear term can be handed by different forms: advective, divergent, skew-symmetric, or rotational (Canuto *et al*., 2006), in spite of being the same mathematically, they present different properties when discretized. The skew-symmetric form is more stable and present best results, but is twice more onerous that the rotational form. However, this inconvenience can be solved using the alternate skew-symmetric form, it is consisting in alternate between the advective and divergent forms in each time step (Souza, 2005),and it is proceeding adopted in the present work.

For all types of handing the non-linear term is necessary solve the convolution integral, but its numerical solution is computational expensive, then the pseudospectral method is used, *i.e.* to calculate the velocity product in the physical space and to transform this product for the spectral space.

When solved numerically the Navier-Stokes equations with the Fourier spectral method using the Discrete Fourier Transform (DFT), which is define by Briggs and Henson (1995):

$$\hat{f}_k = \sum_{n=-N/2+1}^{N/2} f_n e^{\frac{-i2\pi kn}{N}}, \tag{16}$$

where k is wave number, N is number of meshes points, n get the position x_n of collocation points ($x_n = n\Delta x$).

The DFT restriction is periodic boundary conditions, by limiting the use of Fourier spectral transformed for CFD problems. The advantage is low computational cost gives by Fast Fourier Transform (FFT) (Cooley and Tukey, 1965), which solves the DFT (Eq. (16)) of a way numerically efficiently, order *O(Nlog2N)*. For systems with many collocation points, *e.g.* three-dimensional problems, the spectral method is very cheap when compared with another high order methodologies.

2.4. Proposed Methodology: IMERSPEC

The algorithm of IMERSPEC method purposed is:

1) Solve the Eq. (13) in Fourier spectral space, without force term, and obtain the temporal parameter $\hat{u}^*(\vec{k},t)$, using the low dispersion and low storage Runge-Kutta method proposed by Allampalli *et al*., (2009);

2) Use the Inverse Fast Fourier Transformer in $\hat{u}^*(\vec{k},t)$ and obtain $u^*(\vec{x},t)$ at physic space in the domain Ω;

3) Interpolate $u^*(\vec{x},t)$ for the lagrangian domain by cubic function proposed by Griffith and Peskin (2005), and obtain $u^*(\vec{x}_k,t)$;

4) Calculate the lagrangian force, $F_l(\vec{x}_k,t)$, by Eq. (7);

5) Update particles velocity;

6) Distribute the $F_l(\vec{x}_k,t)$ by cubic function proposed by Griffith and Peskin (2005), and obtain $f(\vec{x}_k,t)$ in eulerian domain;

7) Update the eulerian velocity, $u(\vec{x},t)$ by Eq. (8) and transformed it using FFT for spectral space, $\hat{u}^*(\vec{k},t)$, returned by step 1.

2.5. Flow over an immersed body

An inlet profile flow is imposed with uniform velocity U_∞ in [*m/s*] and the flow cross the section of an airfoil (Fig. 4). The flow produces the lift and drag forces. The respectively coefficients of these forces are *Cd* and *Cl*, given by Eqs. (17) and (18). These variables determine the forces that act on bodies immersed in flow. The drag coefficient determines the resistance force of the fluid on the body immersed, while the lift coefficient determines the force that have in the direction perpendicular to incoming flow, the one of the main problems of aeronautical engineering is the optimization of shape of the airfoils, that consist in maximize the lift and minimized the drag of the airfoil profiles.

$$Cd = \frac{-2\sum F_x}{\rho U_\infty^2 c}, \tag{17}$$

$$Cl = \frac{-2\sum F_y}{\rho U_\infty^2 c} \tag{18}$$

where: F_x and F_y are the forces calculated at each lagrangean point obtained by Eq. (7); c is the chord of airfoil.

The calculus domain is divided in 1024x256 collocation points in eulerian domain and 97 points in the lagrangean domain, *i.e.*, the airfoil. The simulations is processed until 75 s of physical time to reach the stead state.

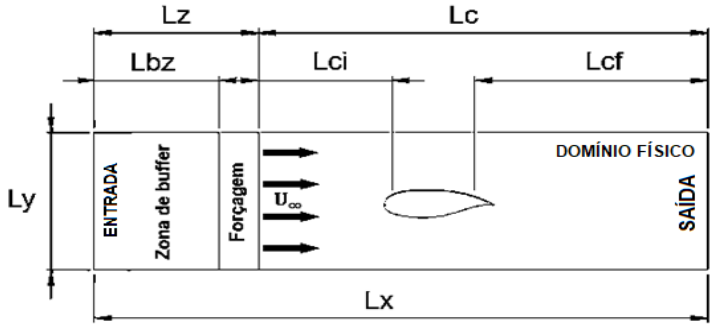

Figure 4. Schematically representation of eulerian and lagrangian domain.

Periodicity conditions were used at the top and bottom boundary of the domain. The inflow condition is a uniform profile of velocity (U_∞*=1,0 m/s*), imposed by immersed boundary. A buffer zone was also used as Uzun, (2003).

The inflow condition is a uniform profile of velocity (U_∞*=1,0 m/s*). Other important parameter is the Reynolds number, in the present work is *Re=1000*. With the Reynolds number is possible to determine the viscosity of the fluid:

$$\nu = \frac{U_\infty c}{Re} \tag{19}$$

4. RESULTS

To validate the use of the IMERSPEC methodology in the numerical simulation of symmetrical airfoils, an analysis of the behavior of an NACA series airfoil was performed, the NACA0012, with a 0.01m chord under a laminar flow for a low Reynolds number (Re = 1000) for different angles of attack ranging from 0 to 30°. A 512x128 Cartesian mesh with 97 points in the lagrangian domain was used and the results were compared with the studies of Kurtulus (2015). Figure 5 presents the mean field of vorticity for an angle of attack of 25°.

Figures 6 and 7 show the average over time of the lift (Cl) and drag (Cd) coefficients, respectively. It is noted that the present study was in good agreement with the results of Kurtulus (2015) until angles of 30º. For angles greater than 30°, the IMERSPEC methodology had a discrepancy among the results, this is due to the fact of the presence of numerical oscillations called Gibbs phenomenon. In the search for better results, new tests are being performed in order to solve these oscillations. The Figure 8 presents the streamlines for different angles of attack, and the results obtained by present work are compared with the results of the Kurtulus' (2015) work.

Figure 5. Mean field of vorticity for an angle of attack of 25°.

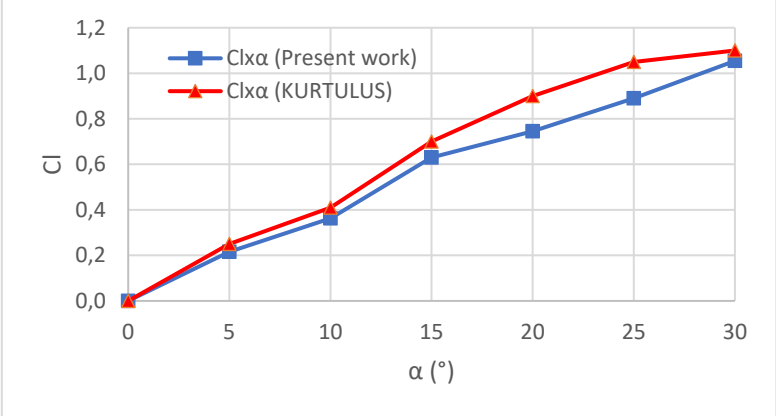

Figure 6. Lift coefficient for different angle of attack.

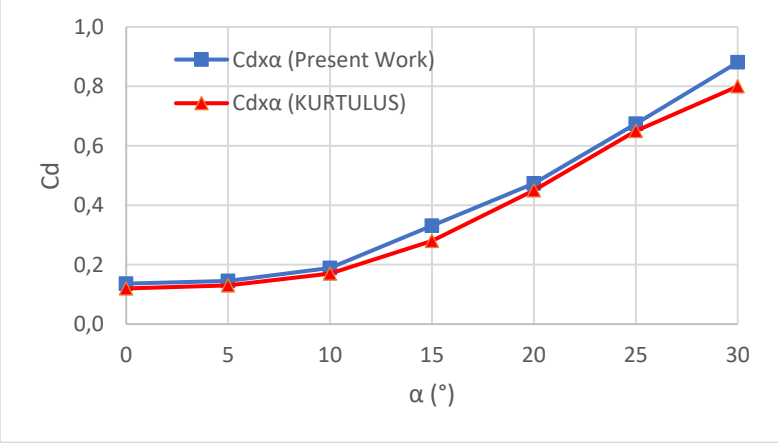

Figure 7. Drag coefficient for different angle of attack.

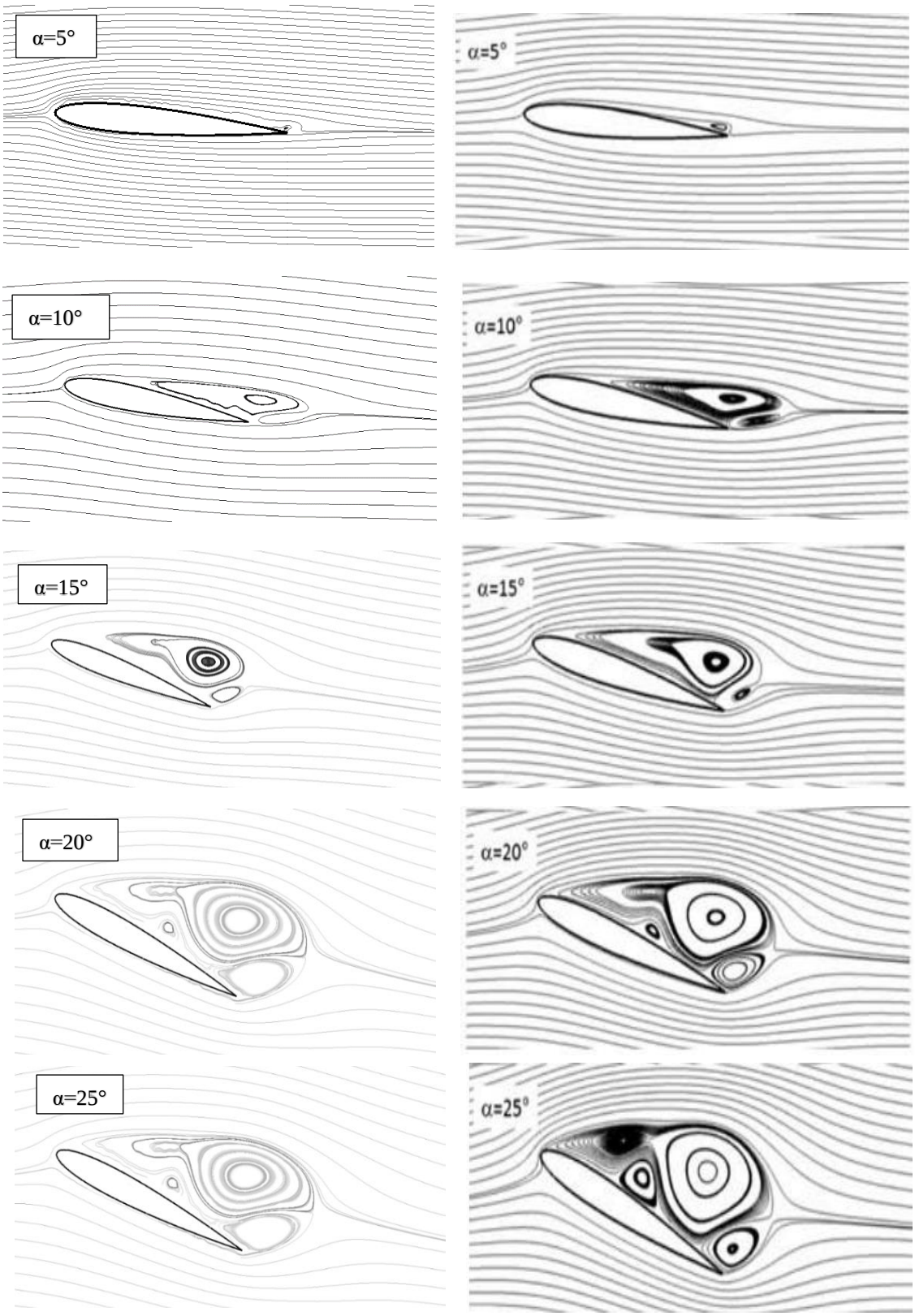

Figure 8. Streamlines for different angles of attack, on the left side are the results obtained by present work and on the right side are the results of the Kurtulus' (2015) work.

5. CONCLUSIONS

The IMERSPEC methodology for the simulation of flow over the airfoil are presented and the results generated in the present work were consistent with the results of Kurtulus (2015). Analyzing the streamlines, the flow instability was expected, and noted the presence of vortices when as the angle of attack increases, due to the shedding of the boundary layer on the upper surface of the airfoil.

The variation of the aerodynamic coefficients in relation to the angle of attack was also presented, until angle of attack 30º the aerodynamic coefficients present good agreement with results of Kurtulus (2015). To angles greater than 30º more investigation is being processed.

6. REFERENCES

Allampalli, V. et al. High-accuracy large-step explicit Runge-Kutta (HALE-RK) schemes for computational aeroacoustics. [S.l.]: J. Comput. Phys., v. 228, 2009. 3837-3850 p.

Briggs, W.; Henson, V. The DFT. Philadelphia: SIAM, 1995.

Canuto, C.; HussainiI, M.Y.; Quarteroni, A.; Zang, T. "A. Spectral methods: Fundamentals in single domains", Spring Verlag, 2006.

Canuto, C.; HussainiI, M.Y.; Quarteroni, A.; Zang, T. "A. Spectral methods: Evolution to complex geometries and applications to fluid dynamics", Springer Verlag, 2007.

Cooley, T. W.; Tukey, J. W. An algorithm for the machine calculation of complex fourier series. Mathematics of Computation, v. 19, p. 297-301, 1965.

Frigo, M., S. G. Johnson. FFTW: An Adaptive Software Architecture for the FFT. Proceedings of the International Conference on Acoustics, Speech, and Signal Processing. Vol. 3, 1998, pp. 1381-1384.

Giannakoglou, K. Design of optimal aerodynamic shapes using stochastic optimization methods and computational intelligence, Progress in Aerospace Sciences, Grécia, v.38, p. 43-76. 2002.

Kurtulus D.F., On the unsteady behavior of the flow around NACA 0012 airfoil with steasy external conditions at Re=1000. Aerospace Engineering Department METU 06800 Ankara, Turkey. 2015.

Mcnughton, J.; Billard, F.; Revell, A. Turbulence modelling of low Reynolds number flow effects around a vertical axis turbine at a range of tip-speed ratios. Journal of Fluids and Structures, v. 47, p. 124 – 138, 2014.

Mariano, F.P. Solução numérica das equações de Navier-Stokes usando uma hibridação das metologias fronteira imersa e pseudo-espectral de Fourier (tese). Faculdade de Engenharia Mecânica, Universidade Federal de Uberlândia – UFU, Uberlândia. 2011.

Monteiro, L. M.; Nascimento, A. A.; Mariano, F. P.; Numerical Shape optimization of airfoil using IMERSPEC and response surface methodologies to flow at low Reynolds number. COMBEM, 2019, COB-2019-2226

Peskin, C.S. Flow patterns around heart calces: A numerical method. Journal of Computational Physics, V. 10, n. 2, p. 252-271, 1972. ISSN 0021-9991.

Shahrokhi, A.; Jahangirian, A. Airfoil shape parameterization for optimum Navier–Stokes design with genetic algorithm, Aerospace Science and Technology Iran, v.11, p.443-450, apr. 2007.

Silveira-Neto, A. Turbulência nos fluidos aplicada. Uberlândia, 2002. Apostila da Disciplina Mecânica dos fluidos do Programa de Pós-Graduação da Universidade Federal de Uberlândia.

Villela, M. F. S. Modelagem Matemática de Escoamentos Bifásicos usando a Metodologia IMERSPEC Combinada com os Métodos VOF e Front-Tracking. Universidade Federal de Uberlândia. Uberlândia. 2015.

7. RESPONSIBILITY NOTICE

The authors are the only responsible for the printed material included in this paper.